

10

Slender rods

The regular object geometries analyzed in the preceding chapter were all three-dimensional, meaning that their sizes in different directions were comparable. Some of the recurring problems in elasticity concern bodies with widely different sizes in different directions. A rod is much thinner than it is long and thus effectively one-dimensional. A plate is much thinner than it is wide, making it effectively two-dimensional. In the mathematical limit a rod becomes a curve described by a vector function of one parameter, while a plate becomes a surface described by a vector function of two parameters.

Mathematics is, however, not physics. The mechanical properties of a rod depend on the shape and size of its cross section and the material from which it is made. The Euler-Bernoulli law for bending and the Coulomb–Saint-Venant law for twisting provide the connection between the mathematical description of a rod’s curvature and torsion and the physical forces and moments at play. As long as the radius of curvature and the torsion length of a rod are much larger than the effective diameter of its cross sections, all the components of the strain tensor will be small. This does, however, not guarantee that the *deflection* of a rod from its initial shape will be small in comparison with the radius of curvature and the torsion length. Thus, for example, the deflection of a longbow is always comparable to its radius of curvature.

The present chapter opens with a discussion of bending with small deflection and no torsion, resulting in a differential equation that can be solved analytically in nearly all practical situations. The chapter continues with an analysis of the famous buckling instability which is encountered when a straight rod is compressed longitudinally and suddenly, spontaneously deviates from its straight shape. Finite deflection without torsion is also tractable and allows us, for example, to calculate the shape of a relaxed stringed bow. Finally, the combination of bending and twisting of rods is analyzed and applied to the case of a coiled spring.

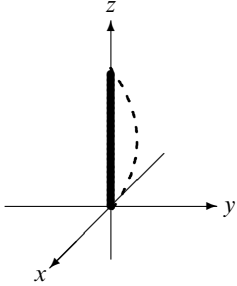
10.1 Small deflections without torsion

Pure bending is an ideal which is rarely met in practice where initially straight beams can be bent and twisted by a multitude of forces. Some forces act locally, like the supports that carry a bridge, others are distributed all over the beam, like the weight of the beam itself. In this section we shall only consider a straight beam or rod, that is bent—but not twisted—by a tiny amount. The beam is, as before, initially placed along the z -axis between $z = 0$ and $z = L$, and bent in the direction of the y -axis by external forces acting only in the yz -plane and external moments only in the direction of the x -axis.

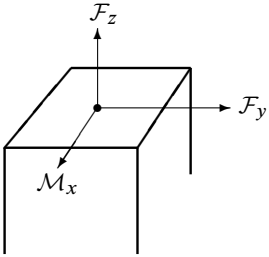
If the beam cross section is not circular, the principal axes of the cross section must be aligned with the x - and y -axes, for otherwise an internal moment will arise along the y -axis (see page 148), which complicates matters. The deformed rod is described by the displacement, $y = y(z)$, of its centroid, also called the deflection of the rod. We shall in this section assume that the deflection varies slowly along the rod, or so that its derivative is small everywhere,

$$\left| \frac{dy}{dz} \right| \ll 1. \quad (10.1)$$

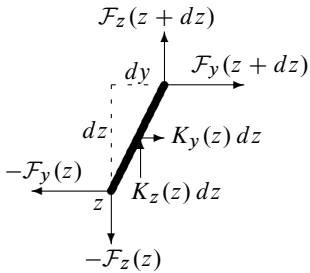
Provided there is a point on the rod which is not deflected, the maximal deflection will always be small compared to the length of the rod, because $|y| \lesssim |dy/dz|_{\max} L \ll L$. Similarly, since $|dy/dz| \lesssim |d^2y/dz^2|_{\max} L \simeq L/R_{\min}$ where R_{\min} is the minimal radius of curvature, this condition also implies that the minimal radius of curvature of the rod should be much larger than its length, $R_{\min} \gg L$.



Initial position of the undeformed beam and a possible planar deflection in the y -direction (dashed).



Forces and moments due to internal stresses in a cross section, here drawn rectangular.



The forces on a small piece of the bent rod. The x -axis comes out of the paper.

Local balance of forces and moments

Consider now the cross section of the bent rod at z . By the assumption of planar bending, the internal stresses in the material makes the part of the rod above this cross section act on the part below with a total transverse force $\mathcal{F}_y(z)$ and a total longitudinal force $\mathcal{F}_z(z)$, as well as a total moment of force $\mathcal{M}_x(z)$, calculated around the centroid of the cross section. Besides these internal forces, there are external forces and moments of force acting on the rod. Some of these act locally in a point, like the pillars of a bridge or the weight of a car on the bridge, others are distributed along the rod, such as the weight of the bridge's material.

Everywhere between the points of attack of external point forces and moments, it is fairly simple to set up the local balance of forces and moments that secure mechanical equilibrium. If $K_y(z)dz$ denotes the transverse resultant of the distributed external forces acting on a small piece dz of the rod, the y -component of the total force on this small piece must vanish, leading to (see the margin figure),

$$\mathcal{F}_y(z + dz) - \mathcal{F}_y(z) + K_y(z) dz = 0,$$

and similarly for the longitudinal distributed force K_z . Dividing by dz we get

$$\boxed{\frac{d\mathcal{F}_y}{dz} = -K_y, \quad \frac{d\mathcal{F}_z}{dz} = -K_z.} \quad (10.2)$$

The total moment of force around the the centroid of the cross section at z must also vanish,

$$\mathcal{M}_x(z + dz) - \mathcal{M}_x(z) + \mathcal{F}_z(z)dy - \mathcal{F}_y(z)dz = 0,$$

and dividing by dz , this equation becomes

$$\boxed{\frac{d\mathcal{M}_x}{dz} = \mathcal{F}_y - \mathcal{F}_z \frac{dy}{dz}.} \quad (10.3)$$

By the assumption, $|dy/dz| \ll 1$, so that the last term on the right may be disregarded, unless the longitudinal force \mathcal{F}_z is much larger than the transverse force \mathcal{F}_y . Everything else being equal, it is the transverse forces \mathcal{F}_y that are important in bending the rod (see also eq. (9.31) on page 150), so for now we drop the longitudinal term on the right, effectively setting $\mathcal{F}_z = 0$.

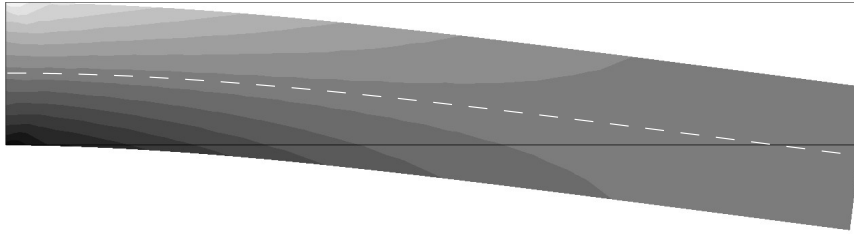


Figure 10.1. Simulation of cantilever bent by its own weight. The undeformed shape is outlined in dark. The cantilever has length $L = 6$ and a quadratic cross section with unit side lengths, yielding an area moment $I = 1/12$. Young’s modulus is $E = 10^4$ and the weight per unit of length $K = 3$. The contours indicate the values of longitudinal stress, σ_{zz} , and clearly show that the rod’s material is stretched on the upper side and compressed at the lower. The dashed white line, which follows the central ray perfectly, is the slender rod prediction (10.8) .

Bending moment

The hypothesis due to Saint-Venant is now that the local bending moment may be obtained from the Euler-Bernoulli law (9.25) with the local curvature given by $\kappa = d^2y/dz^2$, an expression which is correct to order $|dy/dz|^2$. Combining it with force balance (10.2) and moment balance (10.3) (without the longitudinal term), we get the rod equations,

$$\mathcal{M}_x = -EI \frac{d^2y}{dz^2}, \quad \mathcal{F}_y = \frac{d\mathcal{M}_x}{dz}, \quad K_y = -\frac{d\mathcal{F}_y}{dz}. \tag{10.4}$$

Given the transverse distributed force K_y together with suitable boundary conditions, these equations can be solved for the transverse deflections $y(z)$ of a rod. Note that they are valid even if the cross section, the area moment or the material properties change along the rod.

Case: Horizontal uniform rod

For simplicity we now assume that the rod has constant cross section A , constant flexural rigidity EI , and constant mass density ρ . Taking the z -axis to be horizontal and the y -axis pointing downwards along the direction of constant gravity g_0 , the transverse force distribution becomes $K_y \equiv K = \rho A g_0$ and $K_z = 0$. Combining the preceding equations we obtain an amazing fourth-order ordinary differential equation for the deflection,

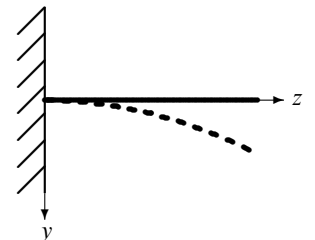
$$EI \frac{d^4y}{dz^4} = K. \tag{10.5}$$

The solution to this equation is a fourth-order polynomial in z with four unknown coefficients,

$$y = a + bz + cz^2 + dz^3 + \frac{K}{24EI}z^4. \tag{10.6}$$

Evidently we need four boundary conditions to determine a solution. We shall now discuss how this works out for a few well-known constructions.

Cantilever bent by its own weight: A cantilever is a horizontal rod that is clamped to a wall at $z = 0$ but free to move at $z = L$. Cantilevers are found in many constructions, for example flagpoles, jumping boards and cranes. At $z = 0$ the clamped state demands that there is no deflection and that the rod is horizontal, such that $y = 0$ and $y' = 0$. In the free



The cantilever is clamped to the wall at one end, but free to move at the other end.

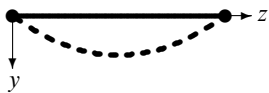
state at $z = L$ there can be no forces or moments, such that $\mathcal{F}_y = 0$ and $M_x = 0$. Since $M_x \sim y''$ and $\mathcal{F}_y \sim y'''$, the full set of boundary conditions are,

$$y(0) = 0, \quad y'(0) = 0, \quad y''(L) = 0, \quad y'''(L) = 0, \quad (10.7)$$

with a prime denoting differentiation with respect to z . One may directly verify that the solution is,

$$y = \frac{K}{24EI} z^2 (z^2 - 4Lz + 6L^2) \quad (10.8)$$

The free end bends down by $y(L) = KL^4/8EI$. As seen in figure 10.1, the slender-rod approximation is quite good even for a not very slender rod.



Bridge supported by hinges at the ends.

Bridge with hinged supports: A bridge is supported at its ends by pylons with hinges that fix the ends but allow them to rotate. In this case the boundary conditions are that there is no displacement and no moments at the ends,

$$y(0) = 0, \quad y''(0) = 0, \quad y(L) = 0, \quad y''(L) = 0. \quad (10.9)$$

The solution is

$$y = \frac{K}{24EI} z(L-z)(L^2 + Lz - z^2). \quad (10.10)$$

In the middle the bridge bends down by $y(L/2) = 5KL^4/384EI$.

Light yoke with heavy loads: Yokes have been used since time immemorial for carrying fairly heavy loads across the shoulders. We idealize the yoke in the form of a straight rod with weight much smaller than the weight of the loads at the extreme ends. These loads must have nearly equal weight W , or the yoke will tip. Disregarding the gravity of the yoke itself ($K \approx 0$) we can view each half of the yoke as a cantilever with boundary conditions

$$y(0) = 0, \quad y'(0) = 0, \quad y''(L) = 0, \quad y'''(L) = -\frac{W}{EI}. \quad (10.11)$$

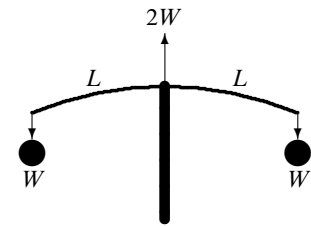
The last condition was obtained from the rod equations (10.4) applied to the end point, $W = \mathcal{F}_y(L) = -EIy'''(L)$. The solution is

$$y(z) = \frac{W}{6EI} z^2 (3L - |z|) \quad \text{for } -L \leq z \leq L. \quad (10.12)$$

Notice that the third derivative jumps from $+W/EI$ to $-W/EI$ when passing upwards through $z = 0$. Something like this actually has to happen. For if there were no jump, the fourth order curve would be completely continuous at $z = 0$, and that is not possible because that would imply no external forces and thus belie the upwards supporting point force $2W$ acting at $z = 0$.

10.2 Buckling instability

A walking stick must be chosen with care. Too sturdy, and it will be heavy and unyielding; too slender, and it may buckle or even collapse under your weight when you lean on it. Stability against buckling and sudden collapse is of course of great technological importance, considering all the struts, columns and girders that are found in human buildings and machines (see figure 10.2). Luckily, however, buckling does not happen until the compressive forces on the beam terminals exceed a certain threshold. First determined by Euler, this threshold load can be used to estimate the point of failure of a column and to set safety limits. Sometimes the buckled rod itself is of technological interest, for example the longbow which may be viewed as a rod brought beyond the buckling threshold and captured in its bent shape by a taught string between its ends.



Yoke with two equal weights W supported in the middle. Each arm of the yoke has length L .



Figure 10.2. Impact buckling of a steel support column in Cortland St./WTC Station (New York City) after the collapse of the World Trade Center on Sept. 11, 2001. Photo by MTA New York City Transit. Permission to be obtained.

Euler's threshold for buckling

In the preceding section we found that the longitudinal force on the rod, \mathcal{F}_z , is only important for small deflections when it is much larger than the transverse force \mathcal{F}_y . In the absence of distributed forces $K_x = K_y = 0$, it follows from (10.2) that \mathcal{F}_y and \mathcal{F}_z are constants along the rod. For simplicity we assume that $\mathcal{F}_y = 0$, so that the rod is only subject to a longitudinal compression force, $\mathcal{F}_z = -\mathcal{F}$, imposed on the upper terminal of the rod (see the margin figure). Integrating local moment balance (10.3) once, we then obtain,

$$EI \frac{d^2 y}{dz^2} = -\mathcal{F} y. \tag{10.13}$$

This relation simply expresses the vanishing of the total moment on the part of the rod below the cross section at z , because the external moment is $-\mathcal{F}y$ and the internal moment $\mathcal{M}_x = -EI d^2 y/dz^2$.

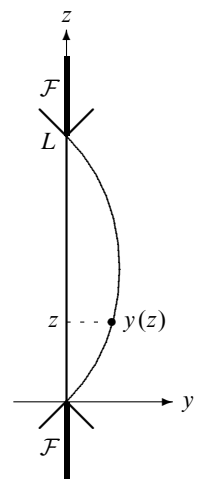
The above is nothing but the standard harmonic equation with wave number $k = \sqrt{\mathcal{F}/EI}$, and its general solution is $y = A \sin kz + B \cos kz$ where A and B are constants. Applying the boundary conditions that $y(0) = y(L) = 0$, the buckling solution becomes,

$$y = A \sin kz, \quad k = \frac{n\pi}{L}, \tag{10.14}$$

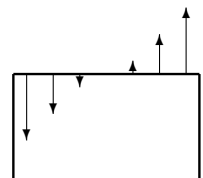
where n is an arbitrary integer. Since $k = \sqrt{\mathcal{F}/EI}$, we arrive at the following expression for the force,

$$\mathcal{F} = k^2 EI = n^2 \frac{\pi^2 EI}{L^2}, \quad \text{for } n = 0, 1, 2, \dots \tag{10.15}$$

Strangely, buckling solutions only exist for certain values of the applied force, corresponding to integer values of n . How should this be understood?



The centroid line of a deformed beam with compressional external forces acting along the z -axis.



Sketch of the stress forces that create the bending couple on the piece of the rod below z . The material is expanded away from the center of curvature and compressed towards it (on the left).

Everyday experience tells us that we can normally lean quite heavily on a walking stick without danger of it buckling. A small force cannot bend the beam but only compress it longitudinally, an effect we have not taken into account in the above calculation. As the applied force \mathcal{F} increases, it will eventually reach the threshold value corresponding to $n = 1$ above, called the *Euler threshold*,

$$\mathcal{F}_E = \frac{\pi^2 EI}{L^2}. \quad (10.16)$$

At this point the longitudinal compression mode becomes unstable and the first buckling solution takes over at the slightest provocation. To prove that this is indeed what takes place requires a stability analysis, which we shall carry out below. In practice only the lowest mode is seen, unless a strong force is rapidly applied, in which case the rod may become permanently deformed, or even crumple and collapse. The buckled column in figure 10.2 appears approximately to be a solution with $n = 2$, permanently frozen into the steel because the yield stress was surpassed in the violent event.

Example 10.1 [Wooden walking stick]: A wooden walking stick has length $L = 1$ m and circular cross section of diameter $2a = 2$ cm. Taking Young's modulus $E = 10^{10}$ Pa and using (9.27), the buckling threshold becomes $\mathcal{F}_E = 775$ N, corresponding to the weight of 79 kg. If you weigh more, it would be prudent to choose a slightly thicker stick. Since the area moment I grows as the fourth power of the radius, increasing the diameter to one inch (2.54 cm) raises the Euler threshold to the weight of 206 kg which should be sufficient for most people.

Stability analysis

Suppose the rod initially is already compressed with a longitudinal terminal force \mathcal{F} and now has the length L . Let us now perturb the straight rod by bending it ever so slightly such that the centroid falls on a chosen curve $y = y(z)$. To do that we need to impose extra (virtual) forces on the rod, and we shall now show that the work of these forces is,

$$W = \frac{1}{2} EI \int_0^L y''(z)^2 dz - \frac{1}{2} \mathcal{F} \int_0^L y'(z)^2 dz. \quad (10.17)$$

The first term is easy, because it represents the pure bending energy of the perturbation obtained from eq. (9.30) with the bending moment $\mathcal{M}_x = -EIy''$. This energy must of course be provided by the work of the virtual forces. The second term arises from the increase in length of the rod due to the perturbation, which releases a bit of the compression energy initially present, and therefore diminishes the amount of work that the virtual forces have to do. Since the perturbation is infinitesimal, we can calculate the (negative) work as $-\mathcal{F}\Delta L$ where ΔL is the increase in length of the perturbed rod. Using that the line element in the yz -plane is

$$d\ell = \sqrt{dy^2 + dz^2} = dz \sqrt{1 + y'(z)^2} \approx dz + \frac{1}{2} y'(z)^2 dz, \quad (10.18)$$

the total increase in length becomes $\Delta L = \int_0^L (d\ell - dz)$ which leads to the second term.

As long as the virtual work W is positive, the undeformed beam is stable when left on its own, because there are no external "agents" around to perform the necessary work. This is evidently the case for $\mathcal{F} = 0$. If, on the other hand, the virtual work W is negative for some choice of $y(z)$, the undeformed beam is unstable and will spontaneously deform without the need of work from any external "agent". Since the second term of (10.17) is always negative for positive \mathcal{F} , the rod will always become unstable for a sufficiently large value of \mathcal{F} . The

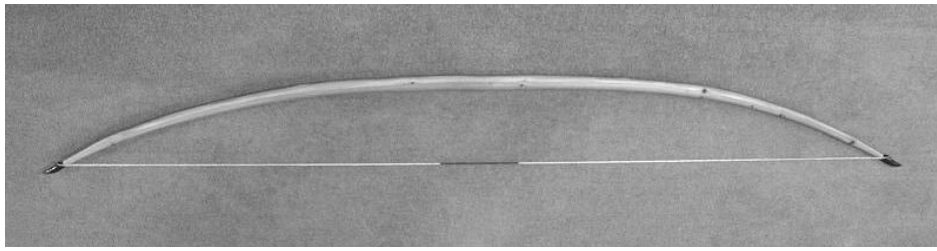


Figure 10.3. English wooden bow. Being visibly thinner towards the ends, this bow does not correspond perfectly to any of the ideal shapes calculated in the text. Reproduced here under Wikimedia Commons License.

lowest possible value, $\mathcal{F} = \mathcal{F}_c$, where this can happen, is called the *critical load*. At this point it takes no work to begin to deform the beam.

The shape of the critical perturbation is determined by that choice of $y(z)$ which yields smallest value of W for a given \mathcal{F} . It can be determined by variation of the perturbation in W , and leads—not unsurprisingly—to the Euler perturbation $y = A \sin kz$ with $k = n\pi/L$. Inserting this solution into (10.17), the integrals are now trivial and we get

$$W = \frac{n^2 \pi^2 A^2}{4L} (n^2 \mathcal{F}_E - \mathcal{F}), \quad (10.19)$$

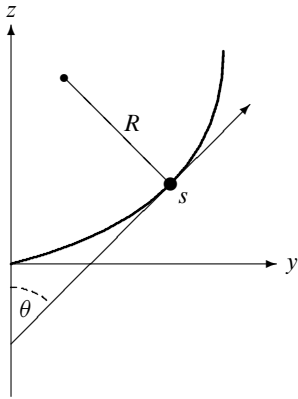
where \mathcal{F}_E is the Euler threshold (10.16). For $F < F_E$ the work is positive for all $n \geq 1$, so that the undeformed beam is stable against any such perturbation. The smallest value of \mathcal{F} at which the work can become zero corresponds to $n = 1$, and this shows that the Euler threshold is the critical load. At this point, the amplitude of the perturbation can grow without requiring us to perform any work on the system. The approximation of small perturbations will, however, soon become invalid, and the rod finds an equilibrium in which it is bent by a finite amount.

10.3 Large deflections without torsion

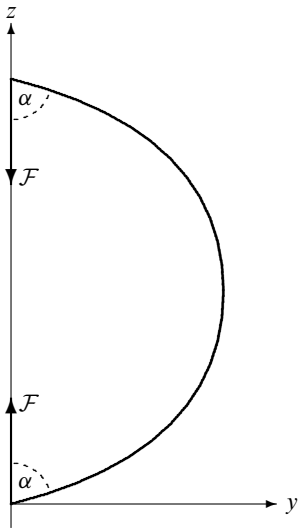
A stringed bow (see figure 10.3) may be viewed as a straight rod that has been brought beyond the buckling threshold and is kept in mechanical equilibrium by the tension in the unstretchable bowstring. In this case, the deflection of the rod is not small compared to the dimension of the bow, but the strains in the material are still small as long as the radius of curvature of the bow is much larger than the transverse dimensions of the beam. In this section we shall develop the formalism for large deflections of the central ray, without torsion and with all bending taking place in a plane. For simplicity we assume that there is no compression or shear in the rod. In the following section we turn towards the general theory of rods with torsion.

Planar deflection

The balance of forces in the yz -plane (10.2) and the bending moment along the x -axis (10.3) are also valid for large planar deflections, where the length and radius of curvature of the rod are comparable. To describe the curved planar rod we use the formalism already introduced for bubble shapes in chapter 5 (page 84) in which the curve is described by the curve length s from one end and the elevation angle, $\theta = \theta(s)$, here chosen relative to the z -axis. From the



The geometry of planar deflection. The curve is parameterized by the arc length s along the curve. A small change in s generates a change in the elevation angle θ determined by the local radius of curvature. With this choice of θ the radius of curvature is negative because θ diminishes when s increases.



The geometry of a stringed bow with opening angle α . It is kept in mechanical equilibrium by a force $\mathcal{F}_z = -\mathcal{F}$ (and $\mathcal{F}_y = 0$).

planar geometry we immediately get the relations (see the margin figure),

$$\frac{dz}{ds} = \cos \theta, \quad \frac{dy}{ds} = \sin \theta, \quad \frac{d\theta}{ds} = -\frac{\mathcal{M}_x}{EI}, \quad (10.20)$$

where we have also used the Euler-Bernoulli law (9.25) to eliminate the radius of curvature, taking into account that a positive moment along x generates a negative curvature.

Differentiating once more with respect to s , and making use of (10.3), it follows that

$$EI \frac{d^2\theta}{ds^2} = -\mathcal{F}_y \cos \theta + \mathcal{F}_z \sin \theta. \quad (10.21)$$

If there are no distributed forces, both \mathcal{F}_y and \mathcal{F}_z are constants. In that case, this equation is a variant of the equation for a mathematical pendulum (page 85). Multiplying by $d\theta/ds$, this equation can immediately be integrated to yield,

$$\frac{1}{2} EI \left(\frac{d\theta}{ds} \right)^2 = -\mathcal{F}_y \sin \theta - \mathcal{F}_z \cos \theta + C \quad (10.22)$$

where C is an integration constant, determined by the boundary conditions. This equation can always be solved by quadrature.

Case: Shape of an ideal stringed bow

The stringed bow (see the margin figure) is kept in mechanical equilibrium by the string force, $\mathcal{F}_z = -\mathcal{F}$, whereas $\mathcal{F}_y = 0$. The ends are hinged such that $d\theta/ds \sim \mathcal{M}_x = 0$ for $z = 0$ and $z = L$. Denoting the opening angle, $\theta = \pm\alpha$, at the ends, this fixes the constant in the integrated equation (10.22), which becomes

$$\left(\frac{d\theta}{ds} \right)^2 = 2k^2 (\cos \theta - \cos \alpha). \quad (10.23)$$

where as before $k = \sqrt{\mathcal{F}/EI}$. Since the angle decreases with s , so that $d\theta/ds < 0$, we find,

$$s = \frac{1}{k} \int_{\theta}^{\alpha} \frac{d\theta'}{\sqrt{2(\cos \theta' - \cos \alpha)}}, \quad (10.24)$$

which is an elliptic integral that is easy to evaluate numerically. For $\theta = -\alpha$ the left hand side becomes equal to the length of the bow L , and this equation provides a relation between $\sqrt{\mathcal{F}/\mathcal{F}_E} = Lk/\pi$ and α .

Finally, we may calculate $dy/d\theta$ and $dz/d\theta$ and integrate to obtain the Cartesian coordinates as functions of the elevation angle θ ,

$$y = \frac{1}{k} \sqrt{2(\cos \theta - \cos \alpha)}, \quad z = \frac{1}{k} \int_{\theta}^{\alpha} \frac{\cos \theta'}{\sqrt{2(\cos \theta' - \cos \alpha)}} d\theta'. \quad (10.25)$$

Together these expressions define the shape of the bow parameterized by θ . In figure 10.4 some shapes are plotted for various opening angles.

Example 10.2 [Wooden longbow]: A certain longbow is constructed from a circular wooden rod of length $L = 150$ cm and diameter $2a = 15$ mm. The bow is stringed with an opening angle of $\alpha = 20^\circ$. The maximal string distance from the bow becomes $d \approx 16$ cm and the stringed height $h \approx 145$ cm. The moment of inertia becomes $I \approx 2.5 \times 10^{-9}$ m⁴, and taking $E = 10$ GPa the Euler threshold becomes $\mathcal{F}_E \approx 109.0$ N, corresponding to a weight of 11 kg which is quite manageable for most people. From the numeric integration we get $\mathcal{F} = 110.6$ N, which is very close to the Euler threshold.

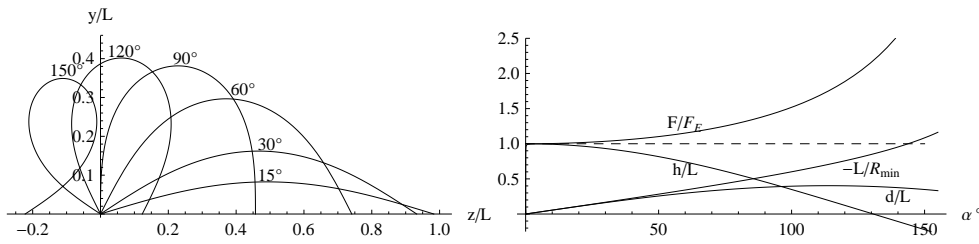
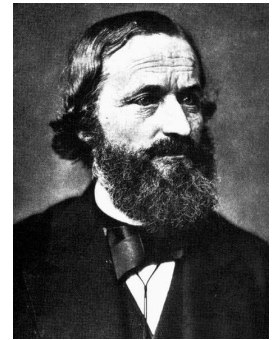


Figure 10.4. Ideal bow shapes (left) for various opening angles . At $\alpha \approx 130^\circ$, the ends of the “bow” cross. Bow parameters (right) as functions of the opening angle. Here h is the distance between the end terminals, d the maximal deflection, and R_{\min} the smallest radius of curvature (at maximal deflection). All lengths are relative to the length L of the bow.

10.4 Mixed bending and twisting

The analysis in the preceding sections can be generalized to arbitrary three-dimensional deformations of rods, including both bending and twisting. We shall again for simplicity assume that the rod is made from a homogeneous, isotropic material, but now we also assume that it has constant circular cross section with radius a and area $A = \pi a^2$. The radius is as before assumed to be so much smaller than the length L of the rod that stretching and shearing can be disregarded, leaving only room for bending and twisting. Since the area moment for twisting is twice the area moment for bending $J = 2I = \frac{\pi}{2}a^4$, we obtain the relation $EI = (1+\nu)\mu J$ between the flexural and torsional rigidities.

The three-dimensional theory of slender rods goes back to Kirchoff (1859). The presentation in this section owes much to [Landau and Lifshitz 1986]. A modern presentation, including rods with non-circular cross sections, can be found in [Bower 2010, ch. 10].



Gustav Robert Kirchoff (1824–1887). German physicist. Developed the famous laws of electrical circuit theory. Founded spectrum analysis (with Bunsen) and applied it to sunlight, using the dark absorption lines to determine its composition. Published a much used 4-volume “Lectures on Mathematical Physics”.

Local balance of forces and moments

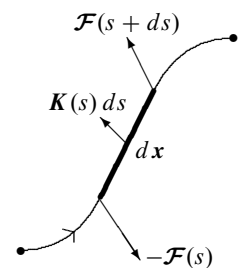
Let the actual shape of the rod’s central ray be given by the vector function $\mathbf{x} = \mathbf{x}(s)$ of the curve length s (the so-called *natural parametrization*). In each circular cross section at s there are internal stresses that integrate up to a total internal force $\mathcal{F}(s)$ and moment of force $\mathcal{M}(s)$. We may as before without loss of generality assume that point-like external forces and moments only act on the end terminals of the rod, because forces or moments acting somewhere between the terminals can be handled by dividing the rod into pieces and imposing suitable continuity conditions where they join. Distributed external forces, for example gravity or viscous drag, act with a vector force $\mathbf{K}(s) ds$ on any infinitesimal piece of the curve between s and $s + ds$. We assume that there are no distributed moments of force.

The balance of forces on a small piece of the rod at rest (see the margin figure) then becomes $\mathcal{F}(s + ds) - \mathcal{F}(s) + \mathbf{K}(s) ds = 0$, or after division with ds ,

$$\boxed{\frac{d\mathcal{F}}{ds} = -\mathbf{K}.} \tag{10.26}$$

Similarly, the balance of moments around the center of the cross section at s takes the form, $\mathcal{M}(s + ds) - \mathcal{M}(s) + d\mathbf{x} \times \mathcal{F}(s + ds) = \mathbf{0}$, and to first order in ds we find,

$$\boxed{\frac{d\mathcal{M}}{ds} = -\frac{d\mathbf{x}}{ds} \times \mathcal{F}.} \tag{10.27}$$

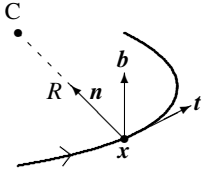


The forces acting on a small nearly straight piece dx of length $ds = |dx|$ of the deformed rod. At the end terminals the missing internal forces and moments must be supplied by external agents.

These are the basic equations that determine the rod shape from the external forces and moments, together with the Euler-Bernoulli and Coulomb-Saint-Venant constitutive equations relating the internal moments to curvature and torsion.

Jean Frédéric Frenet (1816–1900). French mathematician. Only published a few papers and a book. Directed the astronomical observatory in Lyon, and made meteorological observations.

Joseph Alfred Serret (1819–1885). French mathematician. Worked on differential geometry, number theory, and calculus.



The Frenet-Serret basis consists of the tangent vector \mathbf{t} , the normal \mathbf{n} and the binormal \mathbf{b} . The normal points towards the center of curvature C . As the point \mathbf{x} moves along the curve, the basis turns around \mathbf{b} and twists around \mathbf{t} to reflect the geometric curvature and torsion of the oriented curve.

The Frenet-Serret basis

At this point we need to make a small excursion into an efficient mathematical description of the geometry of three-dimensional (spatial) curves, due to Frenet in 1847 (and independently to Serret in 1851). At every point of a curve, a local so-called Frenet-Serret basis is established, starting with the unit *tangent* vector (see the margin figure),

$$\mathbf{t} = \frac{d\mathbf{x}}{ds}. \quad (10.28)$$

The two other unit vectors in this basis are the *normal* \mathbf{n} which points towards the local center of curvature and the *binormal* $\mathbf{b} = \mathbf{t} \times \mathbf{n}$ orthogonal to both. We shall now show that these vectors satisfy the relations,

$$\frac{d\mathbf{t}}{ds} = \kappa \mathbf{n}, \quad \frac{d\mathbf{b}}{ds} = -\tau \mathbf{n}, \quad \frac{d\mathbf{n}}{ds} = \tau \mathbf{b} - \kappa \mathbf{t}. \quad (10.29)$$

where $\kappa = \kappa(s)$ is the *local curvature* and $\tau = \tau(s)$ the *local torsion* of the curve.

Proof: As the point s moves a distance ds along the curve with local curvature $\kappa = 1/R$, the tangent vector rotates towards the center of curvature through an angle $d\phi = ds/R$, such that the change in the tangent vector is $d\mathbf{t} = \mathbf{n} d\phi = \kappa \mathbf{n} ds$. The change $d\mathbf{b}$ in the binormal is orthogonal to \mathbf{b} because \mathbf{b} is a unit vector, but since $d\mathbf{b} = d\mathbf{t} \times \mathbf{n} + \mathbf{t} \times d\mathbf{n} = \mathbf{t} \times d\mathbf{n}$, it is also orthogonal to \mathbf{t} . Consequently, $d\mathbf{b}$ rotates around \mathbf{t} in the direction $-\mathbf{n}$, such that $d\mathbf{b} = -\tau d\psi$ where $d\psi = \tau ds$ is the angle of twist over the distance ds . The last equation follows from $\mathbf{n} = \mathbf{b} \times \mathbf{t}$.

Whereas the curvature κ by definition is never negative, the torsion τ can take both signs. If the curvature vanishes everywhere, $\kappa(s) = 0$, the tangent is constant and the curve becomes straight. In that case torsion can be anything we want and it loses its geometric meaning. If the torsion vanishes everywhere, $\tau(s) = 0$, it follows that \mathbf{b} is a constant, implying that the curve lies in a plane orthogonal to \mathbf{b} . This case was discussed in the preceding section. Generally, it may be shown (see problem 10.8) that the curvature $\kappa(s)$ and the torsion $\tau(s)$ are sufficient to determine the shape $\mathbf{x}(s)$ of the curve, given suitable boundary conditions.

Moments of bending and twisting

Since bending corresponds to a rotation around the binormal and twisting to a rotation around the tangent, we shall assume that the internal moment can only have components along these directions,

$$\mathcal{M} = \mathcal{M}_b \mathbf{b} + \mathcal{M}_t \mathbf{t}. \quad (10.30)$$

This is of course the same as saying that the normal component vanishes, $\mathcal{M}_n = \mathcal{M} \cdot \mathbf{n} = 0$. For a rod with non-circular cross section, \mathcal{M}_n would generally be non-vanishing, even for pure bending.

From moment balance (10.27), we obtain

$$\frac{d\mathcal{M}_b}{ds} \mathbf{b} + \frac{d\mathcal{M}_t}{ds} \mathbf{t} + (\kappa \mathcal{M}_t - \tau \mathcal{M}_b) \mathbf{n} = -\mathbf{t} \times \mathcal{F}.$$

and projecting this equation on the local basis, we get

$$\frac{d\mathcal{M}_b}{ds} = -\mathcal{F}_n, \quad \frac{d\mathcal{M}_t}{ds} = 0, \quad \kappa \mathcal{M}_t - \tau \mathcal{M}_b = \mathcal{F}_b. \quad (10.31)$$

Evidently \mathcal{M}_t must be constant along rod with circular cross section, as long as there are only internal bending and twisting moments. If \mathcal{M}_t is non-zero, the only way that the rod can be twisted is by applying external torsion moments $-\mathcal{M}_t$ and \mathcal{M}_t on the start and end terminals to compensate for the missing internal moments.

Constitutive equations for small deflections

Common experience with highly bendable elastic beams—thin metal wires, electrical cables, garden hoses—tells us that unrestricted twisting and bending can lead to highly contorted shapes. Conversion of twist energy into bending energy may lead to torsional buckling where a part of the rod loops back and writhes around itself [GPL05]. The theory of large deflections of three-dimensional rod shapes is a difficult subject and has been under intense study by physicists and mathematicians since Kirchoff opened the ball.

Paperclips, discussed in example 9.5, and coiled springs like the ones shown in figure 10.5 are examples of slender rods given permanently bent and twisted equilibrium shapes by forces strong enough to overcome the yield stress of the material. The elasticity of such objects under further small deformations around the relaxed equilibrium shapes is often what makes them practically useful: for paperclips to hold sheets of paper together, and for coiled springs to dampen the influence of bumps in the road on the passenger compartments of vehicles, or to slam a mousetrap shut.

Let $\kappa(s)$ and $\tau(s)$ be the geometric curvature and torsion of the relaxed rod with no external load. Under the influence of external forces and moments, the rod deforms into a new equilibrium state, but we assume that the external load is so small that the deflection $\Delta \mathbf{x}(s)$ is everywhere small compared to the radius of curvature $1/\kappa$ and the torsion length $1/\tau$. The constitutive equations are (without proof) assumed to be given by the Euler-Bernoulli law (9.25) and the Coulomb-Saint-Venant law (9.38),

$$\mathcal{M}_b = EI\Delta\kappa, \quad \mathcal{M}_t = \mu J\Delta\tau. \quad (10.32)$$

where $\Delta\kappa(s)$ and $\Delta\tau$ are the (small) changes in curvature and torsion, caused by the external load. The preceding analysis tells us that $\Delta\tau$ must be constant, even if the relaxed state has a frozen-in geometric torsion that varies with s .

10.5 Application: The helical spring

Here we shall only analyze the deformation of a slender circular rod for which the central ray has been permanently shaped into a perfect helix. The helix is uniquely defined by having constant geometric curvature and torsion. It has a beautiful non-trivial regularity that may well be the reason for the fascination it evokes. Everybody has probably made a, not quite perfect, permanent helix by winding a copper wire around a cardboard cylinder, and then removing the cylinder. Helices are found ubiquitously in natural objects—from carbon nanotubes, DNA and bacteria, to horns and vines of large animals and plants—as well as in artificial structures from screws to staircases [CGM06].

Geometry of a perfect helix

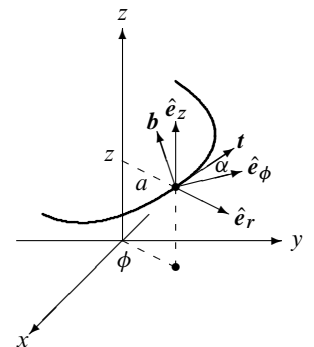
A perfect helix is an infinitely long curve that winds around an imaginary cylinder with constant radius a and constant elevation angle α (see the margin figure). In cylindrical coordinates r , ϕ and z (see appendix D) the natural parametrization of the helix becomes,

$$r = a, \quad \phi = s \frac{\cos \alpha}{a}, \quad z = s \sin \alpha \quad (-\infty < s < \infty). \quad (10.33)$$

In Cartesian coordinates this may be written more compactly,

$$\mathbf{x}(s) = a\hat{\mathbf{e}}_r + s \sin \alpha \hat{\mathbf{e}}_z, \quad (10.34)$$

where $\hat{\mathbf{e}}_r = (\cos \phi, \sin \phi, 0)$, $\hat{\mathbf{e}}_\phi = (-\sin \phi, \cos \phi, 0)$, and $\hat{\mathbf{e}}_z = (0, 0, 1)$ are the usual basis vectors for cylindrical coordinates.



A piece of a right-handed helix with constant radius a and constant elevation angle α , spiraling up along the z -axis. The tangent and binormal of the Frenet-Serret basis are shown.



Figure 10.5. Two kinds of helical springs. On the left, an extension/compression spring, and on the right a torsion spring. Courtesy Spring Solutions Pty Ltd (Australia). Permission to be obtained.

Using that $d\hat{e}_r/d\phi = \hat{e}_\phi$ and $d\hat{e}_\phi/d\phi = -\hat{e}_r$ we find the Frenet-Serret basis,

$$\mathbf{t} = \cos \alpha \hat{e}_\phi + \sin \alpha \hat{e}_z, \quad \mathbf{b} = -\sin \alpha \hat{e}_\phi + \cos \alpha \hat{e}_z, \quad \mathbf{n} = -\hat{e}_r, \quad (10.35)$$

with curvature and torsion,

$$\kappa = \frac{\cos^2 \alpha}{a}, \quad \tau = \frac{\cos \alpha \sin \alpha}{a}. \quad (10.36)$$

Both of these are constant along the helix. The helix is in fact the only curve for which they are both constant (see problem 10.7).

In practice, we would rather describe a finite helical spring of length L by the total turning angle ψ and the height h . These parameters are found by setting $s = L$ in eq. (10.33),

$$\psi = \frac{L \cos \alpha}{a}, \quad h = L \sin \alpha. \quad (10.37)$$

The finite spring thus covers the intervals $0 \leq s \leq L$, $0 \leq \phi \leq \psi$ and $0 \leq z \leq h$. In these variables the curvature and torsion become

$$\kappa = \frac{\psi}{L} \sqrt{1 - \frac{h^2}{L^2}}, \quad \tau = \frac{\psi h}{L^2} \quad (10.38)$$

where we have used that $\cos \alpha = \sqrt{1 - \sin^2 \alpha} = \sqrt{1 - h^2/L^2}$.

Small perfectly helical deflections

The relaxed helix is now deformed by suitable terminal loads to be discussed below. We shall insist that these loads are chosen such that the deformed helix is also a perfect helix with constant parameters $a + \Delta a$ and $\alpha + \Delta \alpha$. Expressed in terms of the change in turning angle $\Delta \psi$ and the change in height Δh , we find from (10.38) the following first-order changes in curvature and torsion,

$$\Delta \kappa = \frac{\Delta \psi}{L} \cos \alpha - \frac{\Delta h}{aL} \sin \alpha, \quad \Delta \tau = \frac{\Delta \psi}{L} \sin \alpha + \frac{\Delta h}{aL} \cos \alpha. \quad (10.39)$$

Inserting these into the constitutive equations the bending and twisting moments become,

$$\mathcal{M}_b = EI \Delta \kappa, \quad \mathcal{M}_t = \mu J \Delta \tau, \quad (10.40)$$

expressed in terms of $\Delta \psi$ and Δh .

Projecting $\mathcal{M} = \mathcal{M}_b \mathbf{b} + \mathcal{M}_t \mathbf{t}$ on the cylindrical directions $\hat{\mathbf{e}}_z$ and $\hat{\mathbf{e}}_\phi$, we get,

$$\mathcal{M}_z = \mathcal{M}_b \cos \alpha + \mathcal{M}_t \sin \alpha, \quad \mathcal{M}_\phi = -\mathcal{M}_b \sin \alpha + \mathcal{M}_t \cos \alpha. \quad (10.41)$$

In terms of the changes in turning angle and height, we have

$$\mathcal{M}_z = A \frac{\Delta\psi}{L} - C \frac{\Delta h}{aL}, \quad \mathcal{M}_\phi = B \frac{\Delta h}{aL} - C \frac{\Delta\psi}{L}, \quad (10.42)$$

where

$$A = EI \cos^2 \alpha + \mu J \sin^2 \alpha, \quad (10.43a)$$

$$B = EI \sin^2 \alpha + \mu J \cos^2 \alpha, \quad (10.43b)$$

$$C = (EI - \mu J) \cos \alpha \sin \alpha \quad (10.43c)$$

All three constants are positive definite because $EI - \mu J = \nu \mu J$ for a circular rod.

Implementation

Since \mathcal{M}_z and \mathcal{M}_ϕ are both independent of s , they determine the external moments that must be applied to the end terminal of the rod at $s = L$. We assume that the start terminal at $s = 0$ is clamped in such a way that it can provide all the necessary reaction forces. The symmetry of the helix indicates that the only possible external load that may lead to a perfectly helical deformation consists of a force $\mathcal{F} = \mathcal{F} \hat{\mathbf{e}}_z$ and a moment $\mathcal{M} = \mathcal{M} \hat{\mathbf{e}}_z$, both acting along the z -axis.

One way of implementing such loads is shown in the margin figure, where a stiff lever transmits both the central external force \mathcal{F} and the central external moment \mathcal{M} to the end terminal. The external force creates a terminal moment $\mathcal{M}_\phi = a\mathcal{F}$, but it appears that the external moment creates a terminal force $\mathcal{F}_\phi = \mathcal{M}/a$. That cannot be right because the total force $\mathcal{F} = \mathcal{F}_z \hat{\mathbf{e}}_z + \mathcal{F}_\phi \hat{\mathbf{e}}_\phi$ has to be constant along the rod according to (10.2) (when there is no distributed load). We shall appeal to Saint-Venant's principle and assume that some diameters away from the rod's terminals we obtain the perfect helix with $\mathcal{M}_\phi = a\mathcal{F}$ and $\mathcal{M}_z = \mathcal{M}$.

Finally, putting it all together, we obtain expressions of the form,

$$\mathcal{F} = k_F \Delta h - m \Delta\psi, \quad \mathcal{M} = k_M \Delta\psi - m \Delta h, \quad (10.44)$$

with spring constants k_F for extension, k_M for torsion and m for "cross-over",

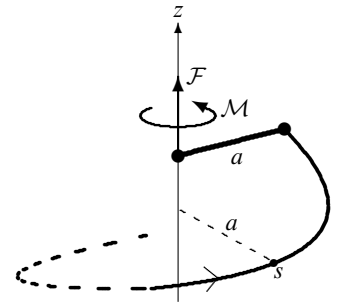
$$k_F = \frac{B}{a^2 L}, \quad k_M = \frac{A}{L}, \quad m = \frac{C}{aL}. \quad (10.45)$$

Note that for small α the force is dominated by the torsional rigidity whereas the moment is dominated by the flexural rigidity. Paradoxically, the elasticity of a coiled compression spring, like the shock absorber in your car, depends mainly on twisting the rod, whereas the elasticity of a torsion spring, like the one in a mousetrap, functions primarily by bending the rod.

Example 10.3 [Locked compression spring]: A helical spring is fixated so that its end terminals cannot turn with respect to each other. Using the expressions for circular rods with rod radius b and $\Delta\psi = 0$, we get

$$k_F = \frac{Eb^4}{8Na^3} \frac{1 + \nu \sin^2 \alpha}{1 + \nu} \cos \alpha, \quad m = -\frac{Eb^4}{8Na^2} \frac{\nu}{1 + \nu} \cos^2 \alpha \sin \alpha. \quad (10.46)$$

where $N = \psi/2\pi$ is the number of turns of the spring.



A possible implementation of the load on the end terminal of a helical spring. The external force \mathcal{F} exerts a pull along the z -axis and the external moment \mathcal{M} wrenches the spring around the z -axis.

The four suspension springs in a certain car have diameter $2a = 10$ cm, rod diameter $2b = 1$ cm, number of turns $N = 5$, and elevation angle $\alpha = 15^\circ$. The length is $L = 163$ cm and the relaxed height $h = 42$ cm. Taking $EE = 200$ GPa, and $\nu = 1/3$, we find the spring constant $k_F = 18.6$ kN/m and the cross-over constant $m = -75$ N. If the passenger compartment (including passengers) has total mass 1000 kg and is suspended by four such springs, we find the compression $\Delta h = -13$ cm and the reaction moment $\mathcal{M} = -10$ Nm.

Problems

10.1 Calculate the buckling threshold for a rod which is only clamped at one end so that it can neither move nor turn.

10.2 Calculate the buckling threshold for a vertical rod, clamped at the bottom and only subject to its own weight.

10.3 Show that (10.21) can always be cast as the equation for the mathematical pendulum when the forces are constants.

10.4 Estimate the shortening of the stringed bow and show that it is negligible for a slender rod.

10.5 Calculate the general shape of a clamped stalk bent by a terminal force.

10.6 Show that the Frenet-Serret basis rotates as a solid body with rotation vector per unit of curve length, $\mathbf{\Omega} = \kappa \mathbf{b} + \tau \mathbf{t}$.

10.7 Prove that if both curvature κ and torsion τ are constants (independent of s), the curve becomes a *perfect helix*.

10.8 Show that the following fourth-order ordinary differential equation is satisfied by any curve $\mathbf{x}(s)$,

$$\frac{d}{ds} \left(\frac{1}{\tau} \frac{d}{ds} \left(\frac{1}{\kappa} \frac{d^2 \mathbf{x}}{ds^2} \right) \right) + \frac{\tau}{\kappa} \frac{d^2 \mathbf{x}}{ds^2} + \frac{d}{ds} \left(\frac{\kappa}{\tau} \frac{d \mathbf{x}}{ds} \right) = \mathbf{0}, \quad (10.47)$$

where $\kappa = \kappa(s)$ and $\tau = \tau(s)$ are the curvature and torsion functions. Discuss the boundary conditions (for, say, $s = 0$) that will determine a unique solution.

10.9 Calculate the elastic behavior of locked torsion spring (with $\Delta h = 0$). Estimate the numeric values of forces and moments involved for a typical mousetrap.

10.10 Show by variation of $x(z)$ that the equation for the minimum of the work functional W is

$$EI \frac{d^4 x}{dz^4} = -F \frac{d^2 x}{dz^2}, \quad (10.48)$$

which is a version of the Euler-Bernoulli equation. Show that this leads to solutions of the form (10.14).